

1

2 **Geochemical and isotopic study of abiotic nitrite reduction coupled to**
3 **biologically produced Fe(II) oxidation in marine environments**

4

5 *Benaiges-Fernandez R.^{a,b,*}, Offeddu F.G.^a, Margalef-Marti R.^{c,d}, Palau J.^{a,c,d}, Urmeneta*
6 *J.^{b,e}, Carrey R.^{c,d}, Otero N.^{c,d,f} and Cama J.^a*

7 ^a Institute of Environmental Assessment and Water Research (IDAEA, CSIC), 08034
8 Barcelona, Catalonia, Spain

9 ^b Departament de Genètica, Microbiologia i Estadística, Universitat de Barcelona, 08028
10 Barcelona, Catalonia, Spain

11 ^c Grup MAiMA, SGR Mineralogia Aplicada, Geoquímica i Geomicrobiologia,
12 Departament de Mineralogia, Petrologia i Geologia Aplicada, Facultat de Ciències de la
13 Terra, Universitat de Barcelona (UB), 08028 Barcelona, Catalonia, Spain

14 ^d Institut de Recerca de l'Aigua (IdRA), Universitat de Barcelona (UB), 08001 Barcelona,
15 Catalonia, Spain

16 ^e Institut de Recerca de la Biodiversitat (IRBio), Universitat de Barcelona, 08028
17 Barcelona, Catalonia, Spain

18 ^f Serra Húnter Fellowship. Generalitat de Catalunya, Catalonia, Spain

19

20 **Corresponding author: robert.benaiges@idaea.csic.es (Robert Benaiges)*

21

22 **Abstract**

23 Estuarine sediments are often characterized by abundant iron oxides, organic matter, and
24 anthropogenic nitrogen compounds (e.g., nitrate and nitrite). Anoxic dissimilatory iron
25 reducing bacteria (e.g., *Shewanella loihica*) are ubiquitous in these environments where
26 they can catalyze the reduction of Fe(III) (oxyhydr)oxides, thereby releasing aqueous
27 Fe(II). The biologically produced Fe(II) can later reduce nitrite to form nitrous oxide.

28 The effect on nitrite reduction by both biologically produced and artificially amended
29 Fe(II) was examined experimentally. Ferrihydrite was reduced by *Shewanella loihica* in a
30 batch reaction with an anoxic synthetic sea water medium. Some of the Fe(II) released by
31 *S. loihica* adsorbed onto ferrihydrite, which was involved in the transformation of
32 ferrihydrite to magnetite. In a second set of experiments with identical medium, no
33 microorganism was present, instead, Fe(II) was amended. The amount of solid-bound Fe(II)
34 in the experiments with bioproducted Fe(II) increased the rate of abiotic NO_2^- reduction
35 with respect to that with synthetic Fe(II), yielding half-lives of 0.07 and 0.47 d,
36 respectively.

37 The $\delta^{18}\text{O}$ and $\delta^{15}\text{N}$ of NO_2^- was measured through time for both the abiotic and
38 inoculated experiments. The ratio of $\epsilon^{18}\text{O}/\epsilon^{15}\text{N}$ was 0.6 for the abiotic experiments and 3.1
39 when NO_2^- was reduced by *S. loihica*, thus indicating two different mechanisms for the
40 NO_2^- reduction. Notably, there is a wide range of the $\epsilon^{18}\text{O}/\epsilon^{15}\text{N}$ values in the literature for
41 abiotic and biotic NO_2^- reduction, as such, the use of this ratio to distinguish between
42 reduction mechanisms in natural systems should be taken with caution. Therefore, we
43 suggest an additional constraint to identify the mechanisms (i.e. abiotic/biotic) controlling
44 NO_2^- reduction in natural settings through the correlation of $\delta^{15}\text{N}-\text{NO}_2^-$ and the aqueous
45 Fe(II) concentration.

46

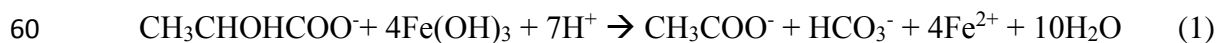
47 *Keywords: iron reducing bacteria, chemodenitrification, nitrite reduction, Fe(II) oxidation, nitrite*
48 *isotope*

49

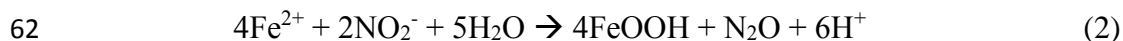
50 1 Introduction

51 Sediments in estuarine and coastal areas often contain terrigenous organic matter and other
52 constituents such as iron and nitrogen compounds (e.g., NO_x), which arrive via rivers and
53 submarine groundwater inputs [1]. Currently, the intensive use of nitrogen-based fertilizers
54 and the systematic release of domestic and industrial waste account for the majority of
55 nitrogen input to these systems [2]. When oxygen is limited in these environments,
56 dissimilatory iron reducing bacteria (e.g., *Shewanella loihica*) are able to reduce Fe(III)
57 (oxyhydr)oxides minerals [3] producing Fe(II) (Eq. 1) [4]. Further, the biologically
58 produced Fe(II) can reduce available nitrite (NO₂⁻) to form nitrous oxide (N₂O) (Eq. 2) [5].

59



61



63

64 Nitrous oxide is a potent greenhouse gas and the single greatest ozone-depleting substance
65 [6]. In recent years, nitrite reduction by Fe(II) oxidation (i.e. chemodenitrification) has been
66 the subject of much research given its environmental relevance [5, 7-10].

67 Both iron and nitrogen cycles are related in anaerobic environments where
68 bioreduction of hydrous ferric oxides (HFO), such as ferrihydrite, leads to nitrite reduction
69 coupled with Fe(II) oxidation [3, 11, 12]. Since nitrite reduction occurs in the presence of
70 aqueous Fe(II) and in the absence of HFO [13, 14], higher abiotic NO₂⁻ reduction rates have
71 been observed in the presence of solid iron phases [5, 15, 16]. Tai and Dempsey (2009)
72 observed higher NO₂⁻ reduction rates when the initial aqueous Fe(II)/HFO ratio was 0.3.
73 They demonstrated that ratio values higher than 0.3 indicate a halt of the reduction even in

74 the presence of mineral-associated Fe(II). Furthermore, they showed that the abiotic NO_2^-
75 reduction was negligible in the absence of HFO. In experiments with aqueous Fe(II) and
76 nitrite, precipitation of HFO or mixed valence (Fe(II), Fe(III)) iron minerals, such as green
77 rust [17], will probably occur due to the oxidation of aqueous Fe(II) [8, 18].

78 Solid Fe(II) (also referred to as structural or solid-bound Fe(II)) may be involved in
79 nitrite reduction [19] together with the dissolved Fe(II). Dhakal et al. (2013) [16] studied
80 the ability of magnetite to reduce nitrite and showed that abiotic NO_2^- reduction by
81 magnetite had a greater impact on nitrite removal than microbially mediated denitrification.
82 However, Lu et al. (2017) [8] showed that magnetite was not able to reduce nitrite in a wide
83 NO_2^- concentration range (30-280 mg L^{-1}) in the absence of solid-bound Fe(II). Few studies
84 on abiotic nitrite reduction in experiments with fresh biogenic magnetite in marine
85 conditions are available to date [20].

86 Currently, the evaluation of abiotic nitrogen reduction coupled with oxidation of
87 Fe(II) in heterogenous systems at laboratory scales has been performed by the addition of
88 synthetic Fe(II) (e.g., FeCl_2) to aqueous solutions with different iron minerals [8, 13, 21].
89 However, in natural settings Fe(II) can derive from microbial reduction of Fe(III)-minerals.
90 Dissimilatory Fe(III) reduction could alter the properties of the iron mineral surface or
91 result in the formation of secondary iron mineral phases such as magnetite or siderite [22].
92 The evaluation of abiotic nitrite reduction therefore requires that experiments be carried out
93 under conditions more comparable to natural settings (e.g., marine environment).

94 In this study, ferrihydrite was the Fe(III) mineral used in biotic and abiotic nitrite
95 reduction experiments with synthetic seawater at pH 8.2 because it is abundant in marine
96 sediments [23] and therefore comparable to natural systems. Fe(II) was either added as

97 FeSO₄ or biologically produced by *Shewanella loihica* (strain PV-4) at similar Fe (II)
98 aqueous concentrations. This strain of *S. loihica* is known to reduce Fe(III) (oxyhydr)oxides
99 in seawater under anoxic conditions [24]. Given its thermodynamic instability and large
100 surface area, ferrihydrite has a high reactivity in the presence of aqueous Fe(II), which may
101 lead to a mineral transformation made up of more crystalline phases containing Fe(II) such
102 as magnetite [25-30].

103 Isotopic analysis is a useful tool for tracing NO_x transformation processes. The
104 enzymatic NO₃⁻ reduction provokes an enrichment in the heavy isotopes of the unreacted
105 substrate [31-34] unlike processes such as dilution that lead to a decrease in concentration
106 without influencing the isotopic ratios. The same pattern is expected for the biotic reduction
107 of all N intermediate products (e.g., NO₂⁻ or N₂O), which will be initially depleted in ¹⁵N
108 and ¹⁸O with respect to the substrate. However, data on the dual N-O isotope systematics
109 during the biotic reduction of intermediate compounds such as NO₂⁻ remain scarce[35, 36].
110 Moreover, two recent isotopic studies on the abiotic NO₂⁻ reduction by Fe(II) found results
111 similar to what is expected from the biotic reaction[7, 9]. Essentially, it is unclear to what
112 degree the isotopic characterization might help in distinguishing biotic and abiotic NO₂⁻
113 reduction. Further studies on the application of isotopic data to elucidate the process
114 controlling the fate of nitrite in natural systems are therefore warranted.

115 In the present study, biotic and abiotic NO₂⁻ reduction experiments using synthetic and
116 biologically produced Fe(II) were performed with anoxic synthetic seawater to (1) shed light
117 on the kinetics of NO₂⁻ reduction in marine environments and (2) evaluate the possible use
118 of isotopic analysis to distinguish between abiotic and biotic (heterotrophic) NO₂⁻

119 reduction. In addition, the reductive dissolution of ferrihydrite by *Shewanella loihica* and
120 the fate of bioproducted Fe(II) was investigated.

121

122 **2 Materials and methods**

123

124 **2.1 Solutions**

125

126 Synthetic sea water (SSW) was prepared to simulate marine sediment conditions following
127 the standard protocol D1141-98 (ATSM International). In addition to this basal medium,
128 10.0 mM of sodium lactate as both a carbon source and electron donor, and 10.0 mM of
129 TRIS-HCl (Tris) as a buffer (pH \approx 8.2) were added. Hereafter, this medium will be referred
130 to as M-SSW.

131 Stock solutions of Fe(II) at pH 1 (HCl) and NO_2^- (230.0 mM 60.0 mM, respectively) were
132 prepared in an anoxic glove box dissolving suitable amounts of FeSO_4 and KNO_2 into
133 nitrogen degassed ultrapure (18.1 M Ω) Milli-Q water. Both solutions were subsequently
134 filtered with a 0.22 μm membrane and stored in sterile bottles.

135 All solutions used in this study were sterilized by autoclave (121 $^\circ\text{C}$, 20 min) unless stated
136 otherwise. Dissolved oxygen concentrations were measured by luminescent dissolved
137 oxygen (LDO) probe (detection limit 0.01 mgL^{-1}).

138 **2.2 Bacterial culture**

139

140 *Shewanella loihica* strain PV-4 was purchased from the German Collection of
141 Microorganisms and Cell Cultures (DSMZ 17748). Bacteria were recovered and cultivated

142 in M1 medium [37] with 10.0 mM of lactate as the electron donor and carbon source and
143 10.0 mM of Fe(III) citrate as the electron acceptor. To obtain bacterial suspensions, cells
144 were cultivated for 24 h and then harvested by centrifugation (5000 rpm for 10 min). The
145 pellet was then re-suspended in SSW. This step was repeated three times as a washing
146 protocol. *S.loihica* was inoculated with a concentration of $1 \cdot 10^7$ colony-forming units (cfu)
147 mL^{-1} .

148

149 **2.3 Ferrihydrite: synthesis and characterization**

150

151 2L-ferrihydrite was synthesized according to a modified protocol of Schwertmann and
152 Cornell (2008) [38] (see supporting information (SI) for more details). The specific surface
153 area was measured by the Brunauer-Emmett-Teller (BET) method [39] with a Gemini 2370
154 surface area analyzer using 5-point N_2 adsorption isotherms. Sample degassing with
155 nitrogen lasted for 2 h at 137 °C. The BET specific surface area measured for unreacted
156 samples varied between 140 and 180 m^2g^{-1} , and for the bioreacted samples it was between
157 144 and 152 m^2g^{-1} .

158 The reacted and unreacted samples were examined by three techniques: (1) scanning
159 electron microscopy (SEM) using a Hitachi H-4100FE instrument under a 15–20 kV
160 potential in a high vacuum and utilizing the backscattered electron detector (BSD) in field
161 emission (FE) and coating the samples with carbon, (2) X-ray diffraction (XRD) using a
162 *PANalytical X'Pert PRO MPD θ/θ* Bragg-Brentano powder diffractometer of 240 mm in
163 radius and Cu $\text{K}\alpha$ radiation ($\lambda = 1.5418 \text{ \AA}$) together with Rietveld analysis to quantify the
164 amount of phases, and (3) Fourier transform infrared spectrometry (FTIR) utilizing a Perkin

165 Elmer frontier / ATR diamond / detector DTGS, accumulation at 16 scans, spectral
166 resolution 4 cm⁻¹, spectral range 4000 - 225 cm⁻¹.

167

168 **2.4 Experimental setup and sampling procedure**

169

170 Table 1 lists the initial experimental conditions. Most of the batch experiments were run in
171 the dark (bottles wrapped with aluminum foil) and in triplicate at 22 ± 2 °C. Bottles
172 (reactors) were placed in an anoxic glove box purged with N₂ and equipped with UV
173 germicidal light for periodic sterilization. Glassware, septa, caps, tips, and media solutions
174 were sterilized by autoclave at 121 °C for 20 min before the experiments.

175

176 **2.4.1 Abiotic nitrite reduction experiments with biologically produced Fe(II)**

177

178 Batch experiments consisted of two stages. In the first stage, no nitrate was
179 amended while Fe(II) was produced biologically (experiment Ferr; Table 1). The anaerobic
180 reductive dissolution of ferrihydrite mediated by *S. loihica* was performed in cultures
181 prepared with the M-SSW medium described above. Bottles of 500 mL were sealed with a
182 screw cap, silicone O-ring and blue butyl rubber stopper before being wrapped in aluminum
183 foil to avoid exposure to light. Autoclaved ferrihydrite powder was put into the bottles
184 (1:100 w/v ratio). Each reactor consisted of a multi-point batch experiment in which the
185 butyl rubber stopper allowed for multiple collection of samples with a syringe over time.
186 Before sampling, the reactors were thoroughly shaken for liquid-solid homogenization.
187 Aliquots of 5 mL were extracted about every 48 h, filtered through a 0.22 µm membrane,

188 and acidified with 200 μL of 6 M HCl solution. One mL was used for immediate Fe(II)
189 analysis, and the remaining 4 mL were stored in the dark at 4 $^{\circ}\text{C}$ for further lactate/acetate
190 measurements.

191 In the second stage, nitrite was amended to the reactors and reduced by the
192 biologically produced Fe(II) (NFerr experiment in Table 1). In other words, the initial
193 conditions of stage two correspond to the final conditions of stage one, in which lactate was
194 consumed and ferrihydrite bioreduction ended. The concentrations of bioproducted Fe(II)
195 and acetate were 1.15 and 8.1 mM, respectively, for at least 10 days. On the tenth day, 4.81
196 mL of a 60.0 mM NO_2^- stock solution were injected into the reactors under anoxic
197 conditions, resulting in a NO_2^- concentration of 0.76 mM. NFerr experiment was performed
198 in duplicate to ensure reproducibility.

199 Three sample aliquots were extracted at each sampling interval: a 5 mL aliquot for
200 aqueous Fe(II) and Fe(III) concentration measurements, another 5 mL aliquot to measure
201 the nitrite isotopic composition ($\delta^{15}\text{N}\text{-NO}_2^-$ and $\delta^{18}\text{O}\text{-NO}_2^-$), and a 1 mL aliquot to measure
202 the NO_2^- concentration. Concentrations of dissolved iron and nitrite were analyzed
203 immediately to prevent measurement error due to subsequent iron oxidation/nitrite
204 reduction. The aliquots taken for isotope analysis were immediately frozen and later
205 defrosted before measurement preparation (Section 2.6).

206

207 **2.4.2 Abiotic nitrite reduction experiments with synthetic Fe(II)**

208

209 To investigate the role of solid and aqueous Fe(II) in nitrite reduction, three abiotic
210 experiments were performed with synthetic Fe(II) in the presence and the absence of

211 ferrihydrite. The $\delta^{15}\text{N}$ and $\delta^{18}\text{O}$ of nitrite were monitored through time. In the experiments
212 containing ferrihydrite, the liquid/solid ratio was the same as in the NFerr experiment.
213 Three distinct experimental conditions were employed: (1) dissolved Fe(II) + NO_2^- without
214 ferrihydrite, (2) ferrihydrite + synthetic Fe(II) (totally solid-bound on by ferrihydrite) +
215 NO_2^- in the absence of aqueous Fe(II) and (3) ferrihydrite + both solid-bound and dissolved
216 Fe(II) + NO_2^- , which are labeled A1, A2, and A3, respectively (Table 1). Three replicates
217 were performed for these experiments. All experiments consisted of a basal medium of
218 SSW supplemented with 10.0 mM acetate and 10.0 mM Tris-HCl buffer. Acetate was
219 added to match the initial conditions in the NFerr experiment (8.1 mM of acetate final
220 concentration; Table 1). Control experiments with autoclaved culture of *Shewanella loihica*
221 were carried out to examine an effect of dead cells on the overall process, and no residual
222 nitrite reduction was observed.

223 In experiment A1, the abiotic reduction of NO_2^- (0.65 mM concentration) by aqueous Fe(II)
224 (1.20 mM concentration) took place in batch reactors with 250 mL of SSW basal solution.
225 The decrease in aqueous Fe(II) and NO_2^- was monitored to evaluate the nitrite reduction
226 rate by implementing a multi-point approach. In multi-point batch experiment A2, reactors
227 contained 2.5 g of ferrihydrite and 250 mL of SSW basal solution amended with Fe (II)
228 (1.20 mM concentration). The aqueous Fe(II) was consumed in 400 min due to its uptake
229 on ferrihydrite (see SI and Fig. S1). Once aqueous Fe(II) was depleted, 3.16 mL of 60.0
230 mM nitrite (0.76 mM concentration) were added to the reactor to promote nitrite reduction
231 by solid-bound Fe(II).

232 The multi-point batch experiment A3 contained 2.5 g of ferrihydrite and significantly more
233 synthetic Fe(II) (2.60 mM final concentration; Table 1) than A2 experiments. Similar to

234 experiment A2, a fast uptake of approximately 1.40 mM Fe(II) occurred, yielding a fairly
235 constant aqueous Fe(II) concentration of approximately 1.20 mM for 8 days. Subsequently,
236 3.16 mL of 60.0 mM of nitrite (0.76 mM final concentration) were injected into the reactor
237 to promote nitrite reduction by oxidation of both solid bound and aqueous Fe(II). Note that
238 the aqueous Fe(II) concentration in the experiments A1, A2, A3 and in the NFerr
239 experiment, previous to the addition of nitrite, were approximately the same (i.e., 1.20
240 mM). The identical sample collection and preservation method used for NFerr was also
241 implemented in experiments A1, A2 and A3 (Section 2.4.1).

242

243 **2.4.3 Biotic nitrite reduction experiments with *S. loihica***

244

245 Bio1 and Bio2 experiments were performed to investigate the heterotrophic nitrite
246 reduction mediated by *S.loihica* in the absence of ferrihydrite and aqueous Fe(II) (Table 1).
247 Each reactor was amended with SSW and adjusted to 10.0 mM of either lactate or acetate
248 as electron donor and carbon source, 10.0 mM of Tris-HCl buffer, and 0.65 nM of nitrite.
249 This enabled the comparison of the biological and abiotic denitrification rates to further
250 characterize of the isotopic signature for each mechanism. Moreover, these experiments
251 allowed an evaluation of the potential contribution of the heterotrophic nitrite reduction in
252 the abiotic experiments with biologically produced Fe(II).

253

254 **2.4.4 Control and adsorption experiments**

255

256 Control reactors with SSW were performed to examine any potential interference between
257 acetate and Fe(II), nitrite and acetate or buffer, acetate and Fe(II) and only nitrite or Fe(II)
258 in SSW (details in SI). Adsorption experiments were carried out to quantify the amount of
259 Fe(II) adsorbed during reductive dissolution of synthesized ferrihydrite (see SI). A Fe(II)
260 adsorption isotherm was performed with increasing concentrations of aqueous Fe(II) in
261 anoxic SSW, acetate and TRIS pH buffer to investigate the mechanisms responsible for the
262 Fe(II) uptake on ferrihydrite (Fig. S2 in SI).

263

264

265 **2.5 Chemical analyses**

266

267 Concentrations of dissolved iron and nitrite were both measured by spectrophotometry (SP-
268 830 PLUS, Metertech Inc.) at wavelengths of 510 nm and 540 nm, respectively. Fe(II) and
269 total iron concentrations were measured immediately after sampling by the phenanthroline
270 method [40]. Nitrite concentration was measured following the method defined by Garcia-
271 Robledo et al. (2004) [41]. The total iron dissolved was also measured using a Perkin-
272 Elmer 3000 inductively coupled plasma optical emission spectrometer (ICP-OES) to
273 confirm that all dissolved iron was in fact Fe(II). Differences in Fe concentrations measured
274 by the phenanthroline method and ICP-OES were smaller than 5%. Concentrations of
275 lactate and acetate were measured by high performance liquid chromatography (Waters 600
276 HPLC pump controller equipped with an Aminex HPX-87H column (300 x 7.8 mm),
277 BioRad column, and a Waters 717plus autoinjector). The associated uncertainty was less
278 than 3 %. The pH of the initial medium was measured in a glove box using a Thermo Orion

279 pH electrode (± 0.02 pH units) and periodically calibrated with standard solutions of pH 2,
280 4 and 7.

281 **2.6 Isotopic analyses**

282

283 $\delta^{15}\text{N-NO}_2^-$ and $\delta^{18}\text{O-NO}_2^-$ were determined following the azide reduction method [42, 43].

284 N_2O was analyzed using a Pre-Con (Thermo Scientific) coupled with a Finnigan MAT 253

285 Isotope Ratio Mass Spectrometer (IRMS, Thermo Scientific). Notation is expressed in

286 terms of delta per mil (δ ‰) (i.e., $\delta = (\text{R}_{\text{sample}} - \text{R}_{\text{standard}}) / \text{R}_{\text{standard}}$, where R is the ratio between

287 the heavy (^{15}N , ^{18}O) and the light (^{14}N , ^{16}O) isotopes) [44]. The $\delta^{15}\text{N}$ and $\delta^{18}\text{S}$ values are

288 reported against international atmospheric N_2 (AIR) and Vienna Standard Mean Oceanic

289 Water (V-SMOW). According to Coplen (2011) [44], several international and laboratory

290 (in-house) standards were interspersed among samples for normalization of analyses. Two

291 international standards (USGS 34 and 35) and two internal laboratory standards (UB-

292 NaNO_3 ($\delta^{15}\text{N} = +16.9$ ‰ and $\delta^{18}\text{O} = +28.5$ ‰) and UB- KNO_2 ($\delta^{15}\text{N} = -28.5$ ‰)) were

293 employed to calibrate the $\delta^{15}\text{N-NO}_2^-$ and $\delta^{18}\text{O-NO}_2^-$ raw values to the international scales.

294 The reproducibility (1σ) of the samples, calculated from the standards systematically

295 interspersed in the analytical batches, was ± 1.0 ‰ for $\delta^{15}\text{N-NO}_2^-$ and ± 1.5 ‰ for $\delta^{18}\text{O-NO}_2^-$.

296 Under closed system conditions, the isotopic fractionation values ($\epsilon^{15}\text{N}_{\text{NO}_2}$ and $\epsilon^{18}\text{O}_{\text{NO}_2}$) are

297 calculated according to the Rayleigh distillation equation:

$$298 \quad \ln \left(\frac{\text{R}_{\text{residual}}}{\text{R}_{\text{initial}}} \right) = \epsilon \times \ln \left(\frac{\text{C}_{\text{residual}}}{\text{C}_{\text{initial}}} \right) \quad (3)$$

299 where ε is the slope of the linear regression between the natural logarithms of the substrate
300 remaining fraction ($\ln(C_{\text{residual}}/C_{\text{initial}})$), where C refers to the analyte concentration, and the
301 determined isotope ratios ($\ln(R_{\text{residual}}/R_{\text{initial}})$), where $R = \delta + 1$.

302 Given that the use of NO_3^- (and NO_2^-) standards to correct $\delta^{18}\text{O}-\text{NO}_2^-$ may cause a bias on
303 their values for the loss of one O atom during NO_3^- to NO_2^- reduction, the results were
304 interpreted according to the changes in the NO_2^- isotopic composition with respect to the
305 initial one.

306 .

307 **3 Results and discussion**

308 **3.1 Bioreduction of ferrihydrite**

309

310 Figure 1 shows the three distinct stages of the bioreduction experiment. In the first
311 stage (approximately 10 days), a significant drop in the initial concentration of lactate (from
312 10.8 to 3.9 mM) was accompanied by a sharp increase in acetate concentration (up to 3.8
313 mM). However, aqueous iron was not detected during this interval. In the second stage
314 (from 10 to 30 days), a gradual decrease in lactate and a progressive increase in acetate
315 were observed together with a significant increase in dissolved iron. In the third stage,
316 lactate was totally depleted after about 60 days, and acetate and Fe(II) concentrations
317 stabilized at 8.1 and 1.15 mM, respectively. The total consumption of lactate (i.e. the
318 electron donor) effectively halted Fe(III)-bioreduction and, therefore, the acetate and
319 aqueous Fe(II) concentrations remained constant.

320 Referring to the bioreduction reaction (Eq. 1), the molar ratio of [acetate]/[lactate] is
321 1. Nevertheless, based on the measured lactate consumption, a 20 % deficit of acetate was
322 observed throughout the experiments (Fig. 1). This non-stoichiometric behavior was mainly
323 attributed to the use of lactate as a carbon source for biomass formation during microbial
324 growth [45]. Further, since the stoichiometric [Fe(II)]/[acetate] ratio is 4 (Eq. 1) and the
325 highest measured concentrations of aqueous Fe(II) and acetate were 1.15 and 8.1 mM,
326 respectively, only a minor fraction of Fe(II) produced (i.e. $\approx 3.5\%$) was found in solution.
327 This Fe(II) deficit could be explained by a large Fe(II) adsorption on ferrihydrite. For
328 instance, Dzombak and Morel (1990) [46] demonstrated that at relatively high pH (e.g. pH
329 ≈ 8.2), ferrihydrite that has a large surface area combined with a poor crystalline
330 organization can cause an exceptionally large sorption capacity of cations. In order to
331 evaluate the Fe(II) adsorption process under the investigated conditions, several Fe(II)-
332 adsorption assays were performed to obtain a Fe(II) adsorption isotherm (Figs. S1 and S2 in
333 SI). The results confirmed a maximum uptake of Fe(II) on ferrihydrite of ≈ 1.20 mM (Fig.
334 S1 in SI) and revealed that, in addition to adsorption, an additional process (ferrihydrite
335 transformation) was responsible for the Fe(II) uptake on ferrihydrite (Fig. S2 in SI).

336 Earlier studies indicated that re-adsorption of Fe(II) on ferrihydrite can result in
337 ferrihydrite transformation to goethite, magnetite or lepidocrocite [27, 29, 30, 47-49]. In
338 addition, the thermodynamic properties of the minerals involved, the aqueous Fe(II)
339 concentration, the biological and physical settings, the presence of humic substances or the
340 design of the experimental setup can play a role in ferrihydrite transformation [49, 50].
341 SEM images (Fig. 2a) show that the surface of the reacted ferrihydrite grains is rougher
342 than that of the unreacted ones. XRD and FTIR analyses of the solid samples before and

343 after the Fe(III) bioreduction process show that ferrihydrite indeed transformed into
344 magnetite ($\text{Fe}^{2+}\text{Fe}^{3+}_2\text{O}_4$) (Fig. 2b,c). Yang et al. (2010) [27] pointed out that this
345 transformation is caused by the inclusion of the biologically produced Fe(II) into the
346 mineral lattice. Figure 2b compares two XRD patterns after performing high statistic wide
347 range scans of pristine and bio-reduced samples. In addition to initial ferrihydrite, two new
348 phases (nanocrystalline magnetite and microcrystalline hematite) were determined to be
349 present in the reacted sample (NFerr experiment) with estimated amounts of 96 wt%
350 (magnetite) and 4 wt% (hematite). The much smaller content of the latter was formed
351 during the ferrihydrite autoclave process [51].

352

353 **3.2 NO_2^- reduction coupled with Fe(II) oxidation**

354

355 Figure 3 shows the evolution through time of the concentrations of nitrite and Fe(II) during
356 abiotic (Fig. 3a-3c) and biotic (Fig. 3d) nitrite reduction. Figure 3a shows the variation in
357 Fe(II) and NO_2^- in a representative A1 experiment with an initial aqueous Fe(II)
358 concentration of ≈ 1.0 mM in the absence of ferrihydrite. After a week, Fe(II) depletion was
359 approximately 50 % of the initial concentration and 35 % of nitrite was reduced. After a
360 month, the Fe(II) depletion was 70 % of the initial concentration and nitrite concentration
361 fell to 65 % of the initial concentration. The average nitrite reduction rate constant (k_{obs})
362 was estimated to be $0.059 \text{ mM}^{-1} \text{ d}^{-1}$ with a half-life value ($t_{1/2}$) of 18.7 d (second-order rate
363 equation (Eq. (S1)) and parameters in Table S2 in SI).

364 Figure 3b depicts the variation in Fe(II) and nitrite concentration in a representative A2
365 experiment in the presence of solid-bound Fe(II) with (i) product magnetite and (ii) Fe(II)

366 adsorbed on the remaining ferrihydrite. About 27 % of the initial NO_2^- was reduced within
367 2 days, indicating that in the absence of aqueous Fe(II), Fe(II) in the solid phase was able to
368 reduce some NO_2^- . After 2 days, the reaction stopped, and nitrite concentration remained
369 constant. An average nitrite reduction rate of $0.22 \text{ mM}^{-1} \text{ d}^{-1}$ was calculated for all replicates
370 (Eq. (S1)) and Table S2 in SI). Figure 3c shows the variation in Fe(II) and nitrite
371 concentration in a representative A3 experiment in the presence of both aqueous Fe(II) and
372 solid bound Fe(II). NO_2^- and aqueous Fe(II) concentrations dropped 13 % and 62 % from
373 the initial value, respectively, within about 2 d, yielding an average nitrite reduction rate of
374 $0.74 \text{ mM}^{-1} \text{ d}^{-1}$ ($t_{1/2} = 0.47 \text{ d}$) (Fig. S4 Table S2 in SI).

375 Figure 3d shows the evolution of bioproducted Fe(II) after the cessation of the
376 Fe(III) reduction in the Ferr experiment (Fig. 1), along with the nitrite concentration added
377 in a representative NFerr experiment. To ensure comparability of the results, the
378 experiment NFerr (Fig. 3d) was selected for its high initial concentration of aqueous
379 bioproducted Fe(II), which was similar to those of the experiments with synthetic Fe(II).
380 Considering the reductive dissolution reaction (Eq. 1) and acetate production, the total
381 concentration of bioproducted Fe(II) was estimated to be 32.0 mM. Nevertheless, the initial
382 concentration of aqueous Fe(II) in the NFerr experiment was 1.20 mM because most of the
383 bioproducted Fe(II) was adsorbed on ferrihydrite and incorporated in to form magnetite (see
384 section 3.1). During the first 2 h, both nitrite and aqueous Fe(II) fell to about 50% and 30%
385 of their initial concentrations, respectively. After 10 h, 87% of the initial nitrite and 38% of
386 the initial aqueous Fe(II) were removed. The nitrite calculated reduction rate was 6.47 mM^{-1}
387 d^{-1} ($t_{1/2} = 0.07 \text{ d}$) (Fig. S4 in SI). In the NFerr experiment with lower concentrations of

388 Fe(II) and nitrite, the rate calculated are within the same range of that from A3 experiment
389 (Table S2 in SI).

390 The *S. loihica* used for the bioproduction of Fe(II) in the Ferr experiment (prior to
391 nitrite addition in the NFerr experiment) could not be eliminated because both autoclave
392 and antibiotics interfered with dissolved Fe(II) (Table S2 in SI). However, as explained in
393 Sections 3.3 and 3.4, the evidence resulting from (i) the isotopic data from the NFerr
394 experiment (Fig. S5 in SI) and (ii) the observed biotic nitrite reduction by *S. loihica* in the
395 Bio1 and Bio2 experiments ruled out any microbial reduction of nitrite.

396 The fastest abiotic nitrite reduction rate was observed in the NFerr experiment
397 where bioproduced Fe(II) was the electron donor. In experiments with synthetic Fe(II), the
398 rate was slower, despite both experiments having similar aqueous Fe(II) concentrations. In
399 experiments with synthetic Fe(II), the nitrite reduction rate was highest in the presence of
400 both aqueous and solid Fe(II) (e.g. A3 experiment), slower in the presence only of solid-
401 bound Fe(II) (e.g. A2 experiment), and slowest in the experiment with only aqueous Fe(II)
402 (e.g. A1 experiment). The highest nitrite reduction rate in the NFerr experiments compared
403 to A3 experiment, both with aqueous and solid-bound Fe(II), suggests that the larger
404 amount of solid-bound Fe(II) obtained in the NFerr experiments could play a crucial role on
405 the nitrite reduction rate. Previous studies suggested that solid-bound Fe(II) is able to
406 reduce nitrite [5, 19, 52], and that an enhanced Fe(II)-rich surface (e.g. magnetite) of
407 bio-reduced Fe(III) (oxyhydr)oxides is able to consume electron acceptors (e.g., toxic
408 hexavalent chromium).

409 The highest nitrite reduction rates were observed in the presence of both aqueous
410 and solid-bound Fe(II). This is in accordance with Gorski and Scherrer (2011) [53] who
411 showed that aqueous Fe(II) removal by iron oxide could affect the reduction potential of the

412 oxide, as a decrease in its oxidation grade leads to an increase in the reducing capacity of
413 the oxide. The difference between the reduction rates calculated in experiments with only
414 solid-phase Fe(II) and experiments containing both solid-phase Fe(II) and dissolved Fe(II)
415 is similar to that calculated in reductive dechlorination by Fe(II)-associated with goethite
416 [54].

417

418

419

420 **3.3 Biotic (heterotrophic) NO₂⁻ reduction by *S. loihica***

421

422 Biotic experiments showed a lag in microbial activity before nitrite reduction commenced.
423 In the reactors amended with lactate, nitrate reduction began after a 1-day lag period. For
424 reactors amended with acetate, nitrite reduction began after a 10-day lag period (Fig. S3 in
425 SI). Yoon et al. (2013) [55] reported a similar behavior for *Shewanella* spp. In contrast,
426 abiotic experiments with bioproducted Fe(II) and acetate, nitrite was consumed in only 10 h
427 (Fig. 3d). These results suggest an absence of microbial nitrite reduction in the abiotic
428 experiments with bioproducted Fe(II). As explained further in Sections 3.4 and 3.5, the
429 isotopic data confirmed that the microbial nitrite reduction can be ruled out in the abiotic
430 nitrite reduction experiments (NFerr experiment).

431 **3.4 Isotopic fractionation during abiotic NO₂⁻ reduction owing to dissolved or solid- 432 bound Fe(II)**

433

434 As is commonly observed for denitrification (sources), the unreacted NO₂⁻ became enriched
435 in the heavy isotopes of N and O (¹⁵N and ¹⁸O) during abiotic nitrate reduction. Table 2 lists

436 the values determined for $\epsilon^{15}\text{N}_{\text{NO}_2}$, $\epsilon^{18}\text{O}_{\text{NO}_2}$ and $\epsilon^{18}\text{O}/\epsilon^{15}\text{N}$ (calculations shown in Fig. S5 in
437 SI). These values are within the range reported in the literature for both the biotic
438 (heterotrophic) and abiotic NO_2^- reductions (Table 3).

439 In the experiments to test the abiotic NO_2^- reduction, differences in NO_2^- isotopic
440 fractionation were not observed (i) when using Fe(II) from biotic or synthetic sources
441 (NFerr and A3 experiments, respectively) nor (ii) when using both aqueous and solid-
442 bound Fe(II) or only aqueous Fe(II) (A1 and A3 experiments, respectively; Table 2). By
443 contrast, in the experiments with solid-bound Fe(II) in the absence of aqueous Fe(II) (A2
444 experiment), the $\epsilon^{15}\text{N}_{\text{NO}_2}$ and $\epsilon^{18}\text{O}_{\text{NO}_2}$ determined were higher (Table 2).

445 In these abiotic NO_2^- reduction experiments, the observed variability of $\epsilon^{15}\text{N}_{\text{NO}_2}$ and
446 $\epsilon^{18}\text{O}_{\text{NO}_2}$ could be caused by the different NO_2^- reduction rates or by a different reaction
447 mechanism during oxidation of dissolved or solid-bound Fe(II). In earlier studies, lower ϵ
448 values have been associated with higher NO_2^- reduction rates [9, 35]. Buchwald et al.
449 (2016) [9] observed differences in ϵ and NO_2^- removal rates using aqueous Fe(II) as
450 electron donor or Fe(II) associated with the oxide surface. However, our results do not
451 show a correlation between the NO_2^- reduction rates and the isotopic fractionation values
452 (Table 2). For instance, $\epsilon^{15}\text{N}_{\text{NO}_2}$ and $\epsilon^{18}\text{O}_{\text{NO}_2}$ were similar in the A3 and NFerr experiments
453 with highly dissimilar NO_2^- reduction rates (0.75 and $6.47 \text{ mM}^{-1} \text{ d}^{-1}$, respectively).

454 The kinetics of the abiotic NO_2^- reduction could be affected by the initial concentration and
455 proportion of the reactants (NO_2^- and Fe(II)), solution pH, and the presence of minerals that
456 were added externally or those precipitated during the reaction [7, 9]. In the latter case, the
457 amount, composition (including the Fe oxidation state) and the mineral specific surface

458 area could have influenced the reaction. In the present study, the formation of secondary
459 magnetite during the Fe(II) oxidation in the Ferr experiment complicates a comparison
460 between the effect of the conditions investigated in this study and earlier studies.

461 Therefore, it is difficult to determine whether the ϵ variability observed is only due to
462 differences in the reduction rates or to the differences in mechanisms (oxidation of aqueous
463 or solid-bound Fe(II) coupled with NO_2^- reduction).

464 A dual element isotope approach was used to further investigate the differences in the ϵ
465 values in the different experiments (Fig. 4). The different slopes (i.e., $\Delta\delta^{18}\text{O}/\Delta\delta^{15}\text{N} \approx$
466 $\epsilon^{18}\text{O}/\epsilon^{15}\text{N}$) suggest the occurrence of different nitrite reduction mechanisms. The higher ϵ
467 values determined in the experiment A2 (solid-bound Fe(II)) compared with the similar
468 values in the NFerr and A3 experiments (aqueous and solid-bound Fe (II)) and the A1
469 experiment (aqueous Fe (II)) suggest that nitrite reduction is controlled by a different
470 mechanism in the presence of only solid-bound Fe(II). Nevertheless, the similar slopes in
471 the dual N-O plot for A1, A2, A3 and NFerr ($\Delta\delta^{18}\text{O}/\Delta\delta^{15}\text{N} = 0.60 \pm 0.02$) indicates a
472 common nitrite reduction mechanism in the abiotic experiments. Further research is needed
473 to elucidate the process controlling the magnitude of ϵ values during nitrite reduction by
474 solid-bound Fe(II).

475 Another consideration in the abiotic NO_2^- reduction experiments is the possible effect of
476 $\delta^{18}\text{O}\text{-NO}_2^-$ equilibration with $\delta^{18}\text{O}\text{-H}_2\text{O}$ on the $\epsilon^{18}\text{O}/\epsilon^{15}\text{N}$ ratio. The magnitude of this effect
477 depends on solution salinity, temperature and/or pH [56]. Buchwald et al. (2016) [9]
478 demonstrated that NO accumulated in a reversible reaction could re-oxidize to NO_2^- by
479 incorporating an O atom from water, which could also influence the $\epsilon^{18}\text{O}/\epsilon^{15}\text{N}$ ratio.

480 Nevertheless, Martin and Casciotti (2016) [36] have shown a negligible effect (0.0035‰)
481 due to equilibrium isotopic exchange at room temperature and pH 7.6 over 2 h between
482 sampling and the azide reaction. Given that our nitrite samples in synthetic seawater were
483 retrieved at pH between 7.8 and 8.2, an oxygen equilibration effect was ruled out. The
484 slopes obtained in the abiotic NO_2^- reduction experiments for relatively short (NFerr
485 experiment) and long (A3 experiment) incubation periods (Table 2 and Fig. 4) reinforce the
486 lack of $\delta^{18}\text{O}\text{-NO}_2^-$ equilibration with $\delta^{18}\text{O}\text{-H}_2\text{O}$.

487 **3.5 Use of isotopic tools to distinguish between abiotic and biotic NO_2^- reduction in the** 488 **field**

489

490 As in the abiotic reduction, a decrease in concentration resulted in an enrichment in the
491 heavy isotopes (^{15}N and ^{18}O) of the unreacted substrate during biotic NO_2^- reduction. The
492 isotopic fractionation results are listed in Table 2 (see calculations in Fig. S5 in SI). NO_2^-
493 reduction by *S. loihica* using lactate as electron donor yielded $\epsilon^{15}\text{N}_{\text{NO}_2} = -1.6 \text{ ‰}$, $\epsilon^{18}\text{O}_{\text{NO}_2} =$
494 -5.3 ‰ and $\epsilon^{18}\text{O}/\epsilon^{15}\text{N} = 3.1$. The $\epsilon^{15}\text{N}_{\text{NO}_2}$ and $\epsilon^{18}\text{O}_{\text{NO}_2}$ obtained are within the range of the
495 values reported in the literature for both the biotic (heterotrophic) and abiotic NO_2^-
496 reduction (Table 3). Nevertheless, under the conditions of these experiments, the value of
497 the isotopic fractionation of nitrogen ($\epsilon^{15}\text{N}_{\text{NO}_2}$) was smaller than those from our abiotic
498 experiments. As a consequence, the value of the $\epsilon^{18}\text{O}/\epsilon^{15}\text{N}$ ratio obtained differs from those
499 calculated for the abiotic experiments (Fig. 4 and Table 2) and becomes higher than prior
500 values reported (Table 3).

501 In the biotic NO_2^- reduction, the magnitude of the $\epsilon^{15}\text{N}_{\text{NO}_2}$ and $\epsilon^{18}\text{O}_{\text{NO}_2}$ values could depend
502 on the enzymes involved, on the NO_2^- transport across the cell and on the NO_2^- reduction
503 rate. However, it is unknown whether the effect of pH or salinity could be negligible on the

504 biotite nitrite reduction as it occurs in the biotic nitrate reduction [57-59]. Bacterial NO_2^-
505 reduction can be catalyzed by two enzymes located in the periplasm (Cu containing NO_2^-
506 reductase encoded as *nirK* (Cu-NIR) and Fe-containing NO_2^- reductase encoded as *nirS*
507 (Fe-NIR) ([60] and references therein). The $\epsilon^{18}\text{O}/\epsilon^{15}\text{N}$ ratio of 3.1 obtained for the biotic
508 NO_2^- reduction by *S. loihica* bears no resemblance to those reported in a study on NO_2^-
509 reduction with different bacterial species. Martin and Casciotti (2016) [36] attributed the
510 variations in the $\epsilon^{18}\text{O}/\epsilon^{15}\text{N}$ ratio to the use of different enzymes since the species with Fe-
511 NIR yielded higher $\epsilon^{18}\text{O}/\epsilon^{15}\text{N}$ ratios (from 0.4 to 1.2) than the species containing Cu-NIR
512 (from 0.05 to 0.2). These authors suggested that Fe-NIR could produce a higher NO_2^- -O
513 isotopic fractionation because it allows cleavage of both N-O bonds since the Fe-NIR
514 catalytic site might bind NO_2^- -N [61, 62]. By contrast, the Cu-NIR catalytic site might bind
515 both the NO_2^- -O atoms and the N-O bond closest to the Asp98 residue, which is cleaved
516 [63, 64], independently of the isotopic composition. The NO_2^- reductase associated with *S.*
517 *loihica* is Cu-NIR [65]. However, our results are not indicative of this hypothesis. Our
518 study showed an $\epsilon^{18}\text{O}_{\text{NO}_2}$ higher than $\epsilon^{15}\text{N}_{\text{NO}_2}$ in contrast to a lower $\epsilon^{18}\text{O}_{\text{NO}_2}$ associated with
519 microorganisms containing Cu-NIR [36].

520 The $\epsilon^{18}\text{O}/\epsilon^{15}\text{N}$ of 3.1 ratio determined for the NO_2^- reduction by *S. loihica* differs from the
521 range obtained for the abiotic experiments (0.6 – 0.7; Fig. 4). Thus, given that *S. loihica* is
522 the only NO_2^- reducing microorganism in our experiments, the $\epsilon^{18}\text{O}/\epsilon^{15}\text{N}$ values calculated
523 in the present study could allow us to distinguish the contribution of the biotic
524 (heterotrophic) and abiotic NO_2^- reductions at the laboratory. However, considering the
525 large variability of the $\epsilon^{18}\text{O}/\epsilon^{15}\text{N}$ ratio (from 0.05 to 3.1) in this study and in the literature
526 for the biotic NO_2^- reduction (Table 2 and Table 3), it would be difficult to distinguish

527 between biotic and abiotic reactions in natural marine environments using this technique.
528 One reason for this is the existence of complex bacterial communities with various NO_2^-
529 reducing enzymes. Another reason is the overlap of biotic $\epsilon^{18}\text{O}/\epsilon^{15}\text{N}$ values with the ones
530 attributed to the abiotic reduction (0.6-2.0; Table 2 and Table 3).

531 Alternatively, the correlation between changes in nitrite isotopic composition ($\Delta\delta^{15}\text{N}_{\text{NO}_2}$ or
532 $\Delta\delta^{18}\text{O}_{\text{NO}_2}$) and dissolved Fe(II) iron concentration ($\ln[\text{Fe(II)}]$) during the abiotic nitrite
533 reduction, could be useful to investigate the process controlling NO_2^- reduction under field
534 conditions. A good correlation between $\delta(^{15}\text{N}$ or $^{18}\text{O})\text{-NO}_2^-$ and $\ln[\text{Fe(II)}]$ in field samples
535 suggests NO_2^- reduction by Fe(II) oxidation, either abiotically or biotically
536 (chemolithotrophically). By contrast, no correlation is expected for heterotrophic NO_2^-
537 reduction. A decrease in Fe(II) concentration coupled with an increase in $\delta^{15}\text{N}_{\text{NO}_2}$ and
538 $\delta^{18}\text{O}_{\text{NO}_2}$ was observed (Fig. 5). In the A1 experiment, the slopes for $\delta^{15}\text{N}_{\text{NO}_2}$ and $\delta^{18}\text{O}_{\text{NO}_2}$ (-
539 5.4 and -3.8, respectively) were lower than those in the A3 (-32.2 and -20.3, respectively)
540 and NFerr experiments (-32.6 and -19.0, respectively). This was due to the higher decrease
541 in aqueous Fe(II) concentrations during the A1 experiment. In contrast to A3 and NFerr,
542 which also contained solid-bound Fe(II) and the total amount of Fe(II) was thus higher than
543 in A1, in the A1 experiment only aqueous Fe(II) was available for nitrite reduction (Table
544 1).

545 Given that the equilibration between $\delta^{18}\text{O}_{\text{NO}_2}$ and $\delta^{18}\text{O}_{\text{H}_2\text{O}}$ could affect $\delta^{18}\text{O}_{\text{NO}_2}$ under
546 natural conditions, only the variation of $\delta^{15}\text{N}_{\text{NO}_2}$ versus Fe(II) concentration could provide
547 reliability of the NO_2^- fate in the environment. However, a possible effect of other N
548 cycling processes (e.g. NO_2^- oxidation to NO_3^- , NO_2^- reduction to NH_4^+ or NH_4^+ oxidation
549 to NO_2^-) on $\delta^{15}\text{N}_{\text{NO}_2}$ should also be considered.

550

551 **4 Conclusions**

552 Experiments simulating an anoxic marine medium were carried out to study nitrite
553 reduction coupled with (bioproducted and synthetic) Fe(II) oxidation. Fe(II) bioproduction
554 was driven by ferrihydrite reduction mediated by *S.loihica*. Fe(II) released was partially re-
555 incorporated into ferrihydrite, which transformed to nanocrystalline magnetite, producing
556 solid Fe(II). Both the bioproducted aqueous Fe(II) and solid Fe(II) played a role in nitrite
557 reduction.

558 Experiments with bioproducted or synthetic Fe(II) (aqueous and solid-bound Fe(II))
559 revealed that abiotic NO₂⁻ reduction is faster in a system with bioproducted Fe(II). The
560 newly formed nano-crystalline magnetite with a high content of solid Fe(II) showed a
561 significant reactivity in the presence of nitrite. Results obtained from the laboratory nitrite
562 reduction experiments using synthetic Fe(II) suggest that with similar concentrations of
563 aqueous Fe(II), nitrite reduction in natural systems could be stronger given the higher
564 amounts of solid-bound Fe(II) obtained in the experiments with bioproducted Fe(II).

565 Experiments with only synthetic Fe(II) (aqueous, solid-bound Fe(II) or both) revealed that
566 in the presence of Fe(II) in both aqueous and solid-bound forms, abiotic NO₂⁻ reduction is
567 faster and more effective in terms of nitrite removal than in the ones with only aqueous
568 Fe(II) or only solid-bound Fe(II).

569 No differences in the $\epsilon^{15}\text{N}_{\text{NO}_2}$ and $\epsilon^{18}\text{O}_{\text{NO}_2}$ were found for the abiotic NO₂⁻ reduction
570 regardless of whether the source of Fe(II) was biotic or synthetic. Differences in $\epsilon^{15}\text{N}_{\text{NO}_2}$ and
571 $\epsilon^{18}\text{O}_{\text{NO}_2}$ were neither found for the abiotic NO₂⁻ reduction by (i) aqueous Fe(II) or (ii)

572 aqueous and solid-bound Fe(II). By contrast, the isotopic fractionation was higher in the
573 experiments with only solid-bound Fe(II). The similar slopes derived in the dual N-O
574 isotope plot ($\epsilon^{18}\text{O}/\epsilon^{15}\text{N} = 0.6$) suggest a sole mechanism controlling the NO_2^- reduction in
575 the abiotic experiments. The higher slope related to the biotic (heterotrophic) experiment
576 ($\epsilon^{18}\text{O}/\epsilon^{15}\text{N} = 3.1$) contrasts with those of the abiotic experiments, becoming one of the
577 highest values reported in the literature.

578 Hence, in laboratory microcosms, which mimic marine environments with *S. loihica* as the
579 only existing NO_2^- -reducing microorganism, the value of the $\epsilon^{18}\text{O}/\epsilon^{15}\text{N}$ ratio allows us to
580 distinguish between the biotic and abiotic NO_2^- reduction. Given the wide range of
581 $\epsilon^{18}\text{O}/\epsilon^{15}\text{N}$ values reported in the literature for the biotic and abiotic NO_2^- reduction by other
582 heterotrophic bacteria, the use of the $\epsilon^{18}\text{O}/\epsilon^{15}\text{N}$ ratio to distinguish different NO_2^- reduction
583 processes in field-scale studies should be discretionally applied.

584 Moreover, the correlation between $\delta^{15}\text{N}_{\text{NO}_2}$ and the natural logarithm of the Fe(II)
585 concentration observed could be used as an additional line of evidence to distinguish
586 between NO_2^- reduction by Fe(II) oxidation, either abiotically or biotically
587 (chemolithotrophically), and heterotrophic bacteria. This observation can improve the
588 prospect of using isotopic data to investigate nitrite reduction processes in the field.

589

590 **5 Acknowledgements**

591 This study was supported by projects CGL2017-87216-C4-1-R, CGL2017-82331-R and
592 CEX2018-000794-S funded by the Spanish Ministry of Science and Innovation and

593 AEI/FEDER funded by the European Union, and by MAG (2017 SGR 1733) financed by
594 the Catalan Government. R. Margalef-Marti wishes to thank the Spanish Government for
595 the Ph.D. grant BES-2015-072882. The authors are indebted to Jordi Bellés (IDAEA-
596 CSIC), Natàlia Moreno (IDAEA-CSIC) and Xavier Alcové (SCTT-Barcelona University)
597 for laboratory assistance and XRD analyses, respectively. The isotopic analyses were
598 prepared at the MAiMA-UB research group laboratory and analyzed at the scientific and
599 technical services of Barcelona University (CCiT-UB). We acknowledge Max Giannetta
600 for his scientific discussions during the manuscript elaboration. We also wish to thank the
601 Editor and three anonymous reviewers for their constructive comments that have improved
602 the quality of the paper.

603

604 6 References

- 605 1. Jani, J. and G.S. Toor, *Composition, sources, and bioavailability of nitrogen in a longitudinal*
606 *gradient from freshwater to estuarine waters*. Water research, 2018. **137**: p. 344-354.
- 607 2. Guerbois, D., et al., *Nitrite reduction by biogenic hydroxycarbonate green rusts: evidence*
608 *for hydroxy-nitrite green rust formation as an intermediate reaction product*.
609 *Environmental science & technology*, 2014. **48**(8): p. 4505-4514.
- 610 3. Melton, E.D., et al., *The interplay of microbially mediated and abiotic reactions in the*
611 *biogeochemical Fe cycle*. Nature Reviews Microbiology, 2014. **12**(12): p. 797-808.
- 612 4. Lovley, D.R., *Dissimilatory Fe (III) and Mn (IV) reduction*. Microbiology and Molecular
613 *Biology Reviews*, 1991. **55**(2): p. 259-287.
- 614 5. Tai, Y.-L. and B.A. Dempsey, *Nitrite reduction with hydrous ferric oxide and Fe (II):*
615 *stoichiometry, rate, and mechanism*. Water research, 2009. **43**(2): p. 546-552.
- 616 6. Ravishankara, A., J.S. Daniel, and R.W. Portmann, *Nitrous oxide (N₂O): the dominant*
617 *ozone-depleting substance emitted in the 21st century*. science, 2009. **326**(5949): p. 123-
618 125.
- 619 7. Grabb, K.C., et al., *A dual nitrite isotopic investigation of chemodenitrification by mineral-*
620 *associated Fe (II) and its production of nitrous oxide*. Geochimica et Cosmochimica Acta,
621 2017. **196**: p. 388-402.
- 622 8. Lu, Y., et al., *Microbial mediated iron redox cycling in Fe (hydr) oxides for nitrite removal*.
623 *Bioresource technology*, 2017. **224**: p. 34-40.
- 624 9. Buchwald, C., et al., *Constraining the role of iron in environmental nitrogen*
625 *transformations: Dual stable isotope systematics of abiotic NO₂⁻ reduction by Fe (II) and*
626 *its production of N₂O*. Geochimica et Cosmochimica Acta, 2016. **186**: p. 1-12.

- 627 10. Carlson, H.K., et al., *Fe (II) oxidation is an innate capability of nitrate-reducing bacteria that*
628 *involves abiotic and biotic reactions*. 2013. **195**(14): p. 3260-3268.
- 629 11. Kampschreur, M.J., et al., *Reduced iron induced nitric oxide and nitrous oxide emission*.
630 *Water Research*, 2011. **45**(18): p. 5945-5952.
- 631 12. Bryce, C., et al., *Microbial anaerobic Fe (II) oxidation—Ecology, mechanisms and*
632 *environmental implications*. 2018. **20**(10): p. 3462-3483.
- 633 13. Robertson, E.K., et al., *Dissimilatory nitrate reduction to ammonium coupled to Fe (II)*
634 *oxidation in sediments of a periodically hypoxic estuary*. *Limnology and Oceanography*,
635 2016. **61**(1): p. 365-381.
- 636 14. Devol, A.H., *Denitrification, anammox, and N₂ production in marine sediments*. Annual
637 review of marine science, 2015. **7**: p. 403-423.
- 638 15. Wu, D., et al., *Denitrification of nitrite by ferrous hydroxy complex: effects on nitrous oxide*
639 *and ammonium formation*. *Chemical Engineering Journal*, 2015. **279**: p. 149-155.
- 640 16. Dhakal, P., et al., *Nitrite reactivity with magnetite*. *Environmental science & technology*,
641 2013. **47**(12): p. 6206-6213.
- 642 17. Pantke, C., et al., *Green rust formation during Fe (II) oxidation by the nitrate-reducing*
643 *Acidovorax sp. strain BoFeN1*. 2012. **46**(3): p. 1439-1446.
- 644 18. Chen, D., et al., *Biological and chemical processes of microbially mediated nitrate-reducing*
645 *Fe (II) oxidation by Pseudogulbenkiania sp. strain 2002*. *Chemical Geology*, 2018. **476**: p.
646 59-69.
- 647 19. Rakshit, S., C.J. Matocha, and M.S. Coyne, *Nitrite reduction by siderite*. *Soil Science Society*
648 *of America Journal*, 2008. **72**(4): p. 1070-1077.
- 649 20. Otte, J.M., et al., *N₂O formation by nitrite-induced (chemo) denitrification in coastal*
650 *marine sediment*. 2019. **9**(1): p. 1-12.
- 651 21. Robertson, E.K. and B. Thamdrup, *The fate of nitrogen is linked to iron (II) availability in a*
652 *freshwater lake sediment*. *Geochimica et Cosmochimica Acta*, 2017. **205**: p. 84-99.
- 653 22. Roh, Y., et al., *Metal reduction and iron biomineralization by a psychrotolerant Fe (III)-*
654 *reducing bacterium, Shewanella sp. strain PV-4*. *Appl. Environ. Microbiol.*, 2006. **72**(5): p.
655 3236-3244.
- 656 23. Canfield, D.E., *Reactive iron in marine sediments*. *Geochimica et Cosmochimica Acta*, 1989.
657 **53**(3): p. 619-632.
- 658 24. Benaiges-Fernandez, R., et al., *Dissimilatory bioreduction of iron (III) oxides by Shewanella*
659 *loihica under marine sediment conditions*. *Marine environmental research*, 2019. **151**: p.
660 104782.
- 661 25. Tomaszewski, E.J., et al., *The role of dissolved Fe (II) concentration in the mineralogical*
662 *evolution of Fe (hydr) oxides during redox cycling*. *Chemical Geology*, 2016. **438**: p. 163-
663 170.
- 664 26. Boland, D.D., et al., *Effect of solution and solid-phase conditions on the Fe (II)-accelerated*
665 *transformation of ferrihydrite to lepidocrocite and goethite*. *Environmental science &*
666 *technology*, 2014. **48**(10): p. 5477-5485.
- 667 27. Yang, L., et al., *Kinetics of Fe (II)-catalyzed transformation of 6-line ferrihydrite under*
668 *anaerobic flow conditions*. *Environmental science & technology*, 2010. **44**(14): p. 5469-
669 5475.
- 670 28. Yee, N., et al., *The rate of ferrihydrite transformation to goethite via the Fe (II) pathway*.
671 *American Mineralogist*, 2006. **91**(1): p. 92-96.
- 672 29. Hansel, C.M., et al., *Secondary mineralization pathways induced by dissimilatory iron*
673 *reduction of ferrihydrite under advective flow*. *Geochimica et Cosmochimica Acta*, 2003.
674 **67**(16): p. 2977-2992.

- 675 30. Piepenbrock, A., et al., *Dependence of microbial magnetite formation on humic substance*
676 *and ferrihydrite concentrations*. *Geochimica et Cosmochimica Acta*, 2011. **75**(22): p. 6844-
677 6858.
- 678 31. Böttcher, J., et al., *Using isotope fractionation of nitrate-nitrogen and nitrate-oxygen for*
679 *evaluation of microbial denitrification in a sandy aquifer*. *Journal of Hydrology*, 1990.
680 **114**(3-4): p. 413-424.
- 681 32. Fukada, T., et al., *A dual isotope approach to identify denitrification in groundwater at a*
682 *river-bank infiltration site*. *Water Research*, 2003. **37**(13): p. 3070-3078.
- 683 33. Mariotti, A., et al., *Experimental determination of nitrogen kinetic isotope fractionation:*
684 *some principles; illustration for the denitrification and nitrification processes*. *Plant and*
685 *soil*, 1981. **62**(3): p. 413-430.
- 686 34. Aravena, R. and W.D. Robertson, *Use of multiple isotope tracers to evaluate denitrification*
687 *in ground water: Study of nitrate from a large-flux septic system plume*. *Groundwater*,
688 1998. **36**(6): p. 975-982.
- 689 35. Bryan, B.A., et al., *Variable expression of the nitrogen isotope effect associated with*
690 *denitrification of nitrite*. *Journal of Biological Chemistry*, 1983. **258**(14): p. 8613-8617.
- 691 36. Martin, T.S. and K.L. Casciotti, *Nitrogen and oxygen isotopic fractionation during microbial*
692 *nitrite reduction*. *Limnology and Oceanography*, 2016. **61**(3): p. 1134-1143.
- 693 37. Gao, H., et al., *Shewanella loihica sp. nov., isolated from iron-rich microbial mats in the*
694 *Pacific Ocean*. *International Journal of Systematic and Evolutionary Microbiology*, 2006.
695 **56**(8): p. 1911-1916.
- 696 38. Schwertmann, U. and R.M. Cornell, *Iron oxides in the laboratory: preparation and*
697 *characterization*. 2008: John Wiley & Sons.
- 698 39. Brunauer, S., P.H. Emmett, and E. Teller, *Adsorption of gases in multimolecular layers*.
699 *Journal of the American chemical society*, 1938. **60**(2): p. 309-319.
- 700 40. Stucki, J., *The Quantitative Assay of Minerals for Fe²⁺ and Fe³⁺ Using 1, 10-*
701 *Phenanthroline: II. A Photochemical Method*. *Soil Science Society of America Journal*, 1981.
702 **45**(3): p. 638-641.
- 703 41. García-Robledo, E., A. Corzo, and S. Papaspyrou, *A fast and direct spectrophotometric*
704 *method for the sequential determination of nitrate and nitrite at low concentrations in*
705 *small volumes*. *Marine Chemistry*, 2014. **162**: p. 30-36.
- 706 42. McIlvin, M.R. and M.A. Altabet, *Chemical conversion of nitrate and nitrite to nitrous oxide*
707 *for nitrogen and oxygen isotopic analysis in freshwater and seawater*. *Analytical*
708 *Chemistry*, 2005. **77**(17): p. 5589-5595.
- 709 43. Ryabenko, E., M.A. Altabet, and D.W. Wallace, *Effect of chloride on the chemical*
710 *conversion of nitrate to nitrous oxide for $\delta^{15}N$ analysis*. *Limnology and Oceanography:*
711 *Methods*, 2009. **7**(7): p. 545-552.
- 712 44. Coplen, T.B., *Guidelines and recommended terms for expression of stable-isotope-ratio and*
713 *gas-ratio measurement results*. *Rapid communications in mass spectrometry*, 2011.
714 **25**(17): p. 2538-2560.
- 715 45. Lanthier, M., K.B. Gregory, and D.R. Lovley, *Growth with high planktonic biomass in*
716 *Shewanella oneidensis fuel cells*. *FEMS microbiology letters*, 2008. **278**(1): p. 29-35.
- 717 46. Dzombak, D.A. and F.M. Morel, *Surface complexation modeling: hydrous ferric oxide*.
718 1990: John Wiley & Sons.
- 719 47. Xiao, W., et al., *Use of fourier transform infrared spectroscopy to examine the Fe (II)-*
720 *Catalyzed transformation of ferrihydrite*. *Talanta*, 2017. **175**: p. 30-37.

- 721 48. Xiao, W., et al., *Effect of Shewanella oneidensis on the kinetics of Fe (II)-catalyzed*
722 *transformation of ferrihydrite to crystalline iron oxides*. Environmental science &
723 technology, 2018. **52**(1): p. 114-123.
- 724 49. Dippon, U., et al., *Secondary mineral formation during ferrihydrite reduction by Shewanella*
725 *oneidensis MR-1 depends on incubation vessel orientation and resulting gradients of cells,*
726 *Fe²⁺ and Fe minerals*. Geomicrobiology Journal, 2015. **32**(10): p. 878-889.
- 727 50. Amstaetter, K., T. Borch, and A.J.G.e.C.A. Kappler, *Influence of humic acid imposed*
728 *changes of ferrihydrite aggregation on microbial Fe (III) reduction*. 2012. **85**: p. 326-341.
- 729 51. Das, S., M.J. Hendry, and J. Essilfie-Dughan, *Transformation of two-line ferrihydrite to*
730 *goethite and hematite as a function of pH and temperature*. Environmental science &
731 technology, 2011. **45**(1): p. 268-275.
- 732 52. Byrne, J., et al., *Control of nanoparticle size, reactivity and magnetic properties during the*
733 *bioproduction of magnetite by Geobacter sulfurreducens*. Nanotechnology, 2011. **22**(45):
734 p. 455709.
- 735 53. Gorski, C.A. and M.M. Scherer, *Fe²⁺ sorption at the Fe oxide-water interface: A revised*
736 *conceptual framework*, in *Aquatic Redox Chemistry*. 2011, ACS Publications. p. 315-343.
- 737 54. Elsner, M., et al., *Reactivity of Fe (II)-bearing minerals toward reductive transformation of*
738 *organic contaminants*. 2004. **38**(3): p. 799-807.
- 739 55. Yoon, S., R.A. Sanford, and F.E. Löffler, *Shewanella spp. use acetate as an electron donor*
740 *for denitrification but not ferric iron or fumarate reduction*. Appl. Environ. Microbiol.,
741 2013. **79**(8): p. 2818-2822.
- 742 56. Buchwald, C. and K.L. Casciotti, *Isotopic ratios of nitrite as tracers of the sources and age of*
743 *oceanic nitrite*. Nature Geoscience, 2013. **6**(4): p. 308-313.
- 744 57. Granger, J., et al., *Nitrogen and oxygen isotope fractionation during dissimilatory nitrate*
745 *reduction by denitrifying bacteria*. Limnology and Oceanography, 2008. **53**(6): p. 2533-
746 2545.
- 747 58. Wunderlich, A., R. Meckenstock, and F. Einsiedl, *Effect of different carbon substrates on*
748 *nitrate stable isotope fractionation during microbial denitrification*. Environmental science
749 & technology, 2012. **46**(9): p. 4861-4868.
- 750 59. Chen, G., et al., *Dual nitrogen-oxygen isotopic analysis and kinetic model for enzymatic*
751 *nitrate reduction coupled with Fe (II) oxidation by Pseudogulbenkiania sp. strain 2002*.
752 2020. **534**: p. 119456.
- 753 60. Kuypers, M.M., H.K. Marchant, and B. Kartal, *The microbial nitrogen-cycling network*.
754 Nature Reviews Microbiology, 2018. **16**(5): p. 263.
- 755 61. Fülöp, V., et al., *The anatomy of a bifunctional enzyme: structural basis for reduction of*
756 *oxygen to water and synthesis of nitric oxide by cytochrome cd1*. Cell, 1995. **81**(3): p. 369-
757 377.
- 758 62. Maia, L.B. and J.J. Moura, *How biology handles nitrite*. Chemical reviews, 2014. **114**(10): p.
759 97.
- 760 63. Li, Y., M. Hodak, and J. Bernholc, *Enzymatic mechanism of copper-containing nitrite*
761 *reductase*. Biochemistry, 2015. **54**(5): p. 1233-1242.
- 762 64. Murphy, M.E., S. Turley, and E.T. Adman, *Structure of nitrite bound to copper-containing*
763 *nitrite reductase from Alcaligenes faecalis mechanistic implications*. Journal of Biological
764 Chemistry, 1997. **272**(45): p. 28455-28460.
- 765 65. Simpson, P.J., D.J. Richardson, and R. Codd, *The periplasmic nitrate reductase in*
766 *Shewanella: the resolution, distribution and functional implications of two NAP isoforms,*
767 *NapEDABC and NapDAGHB*. Microbiology, 2010. **156**(2): p. 302-312.

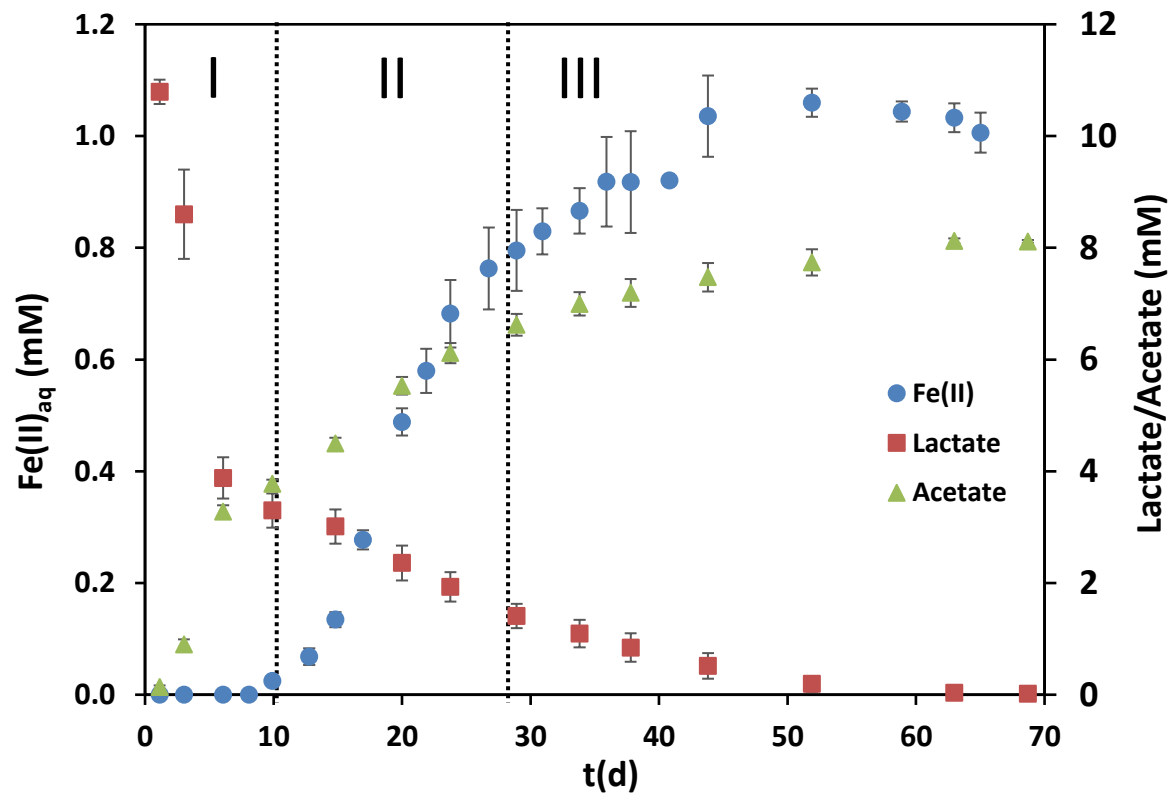
Figure 1

Figure 2

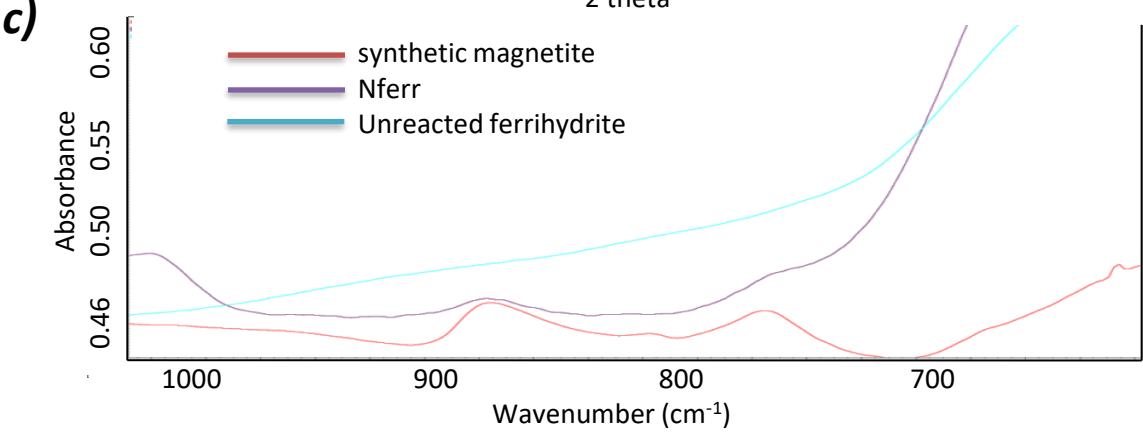
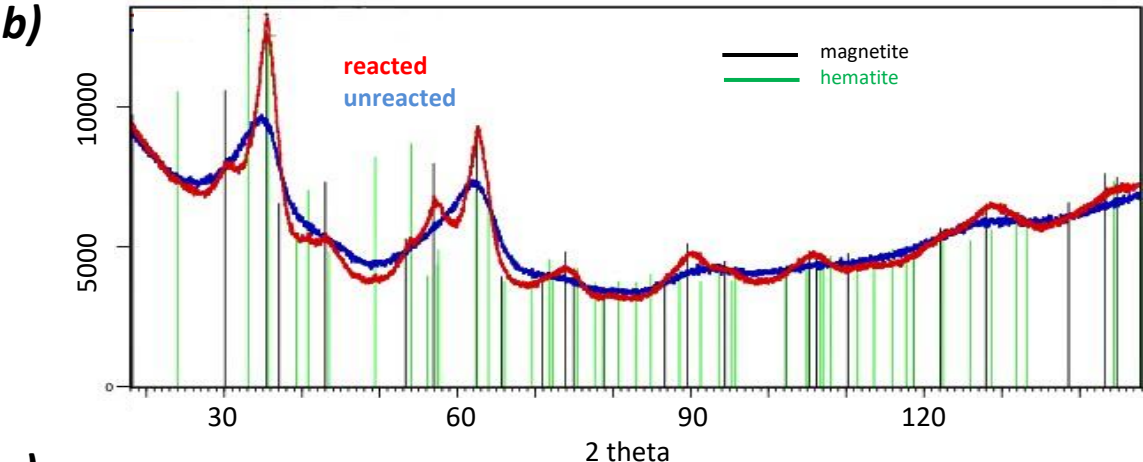
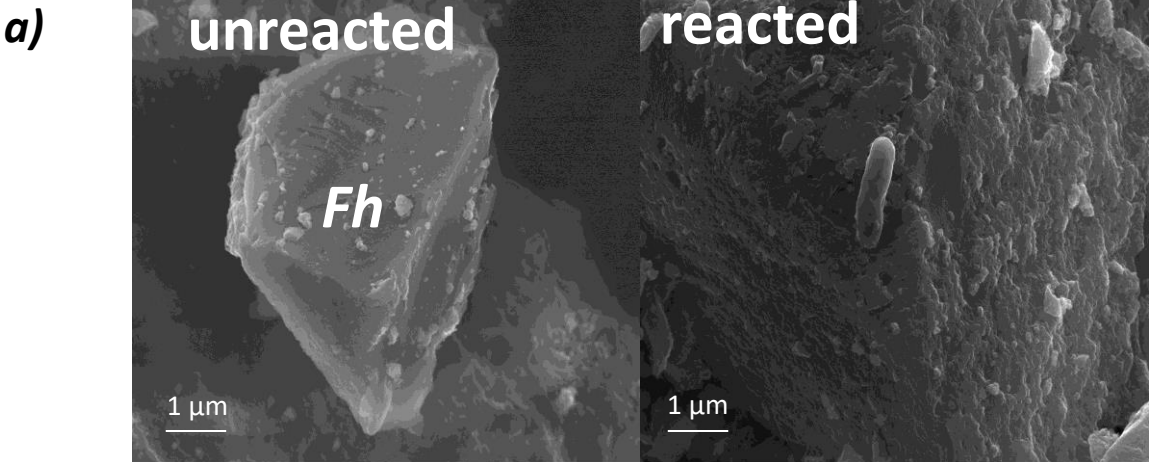


Figure 3

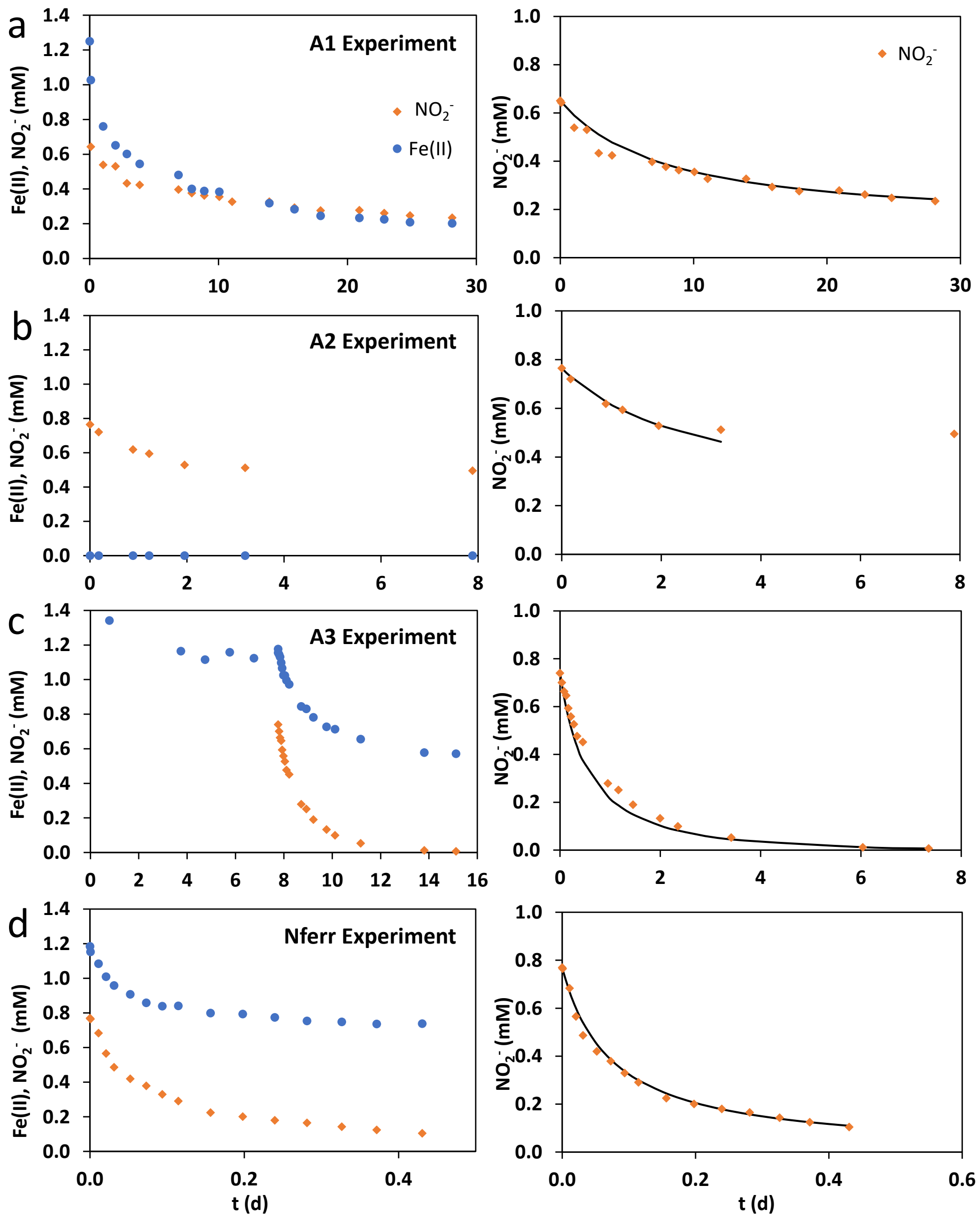


Figure 4

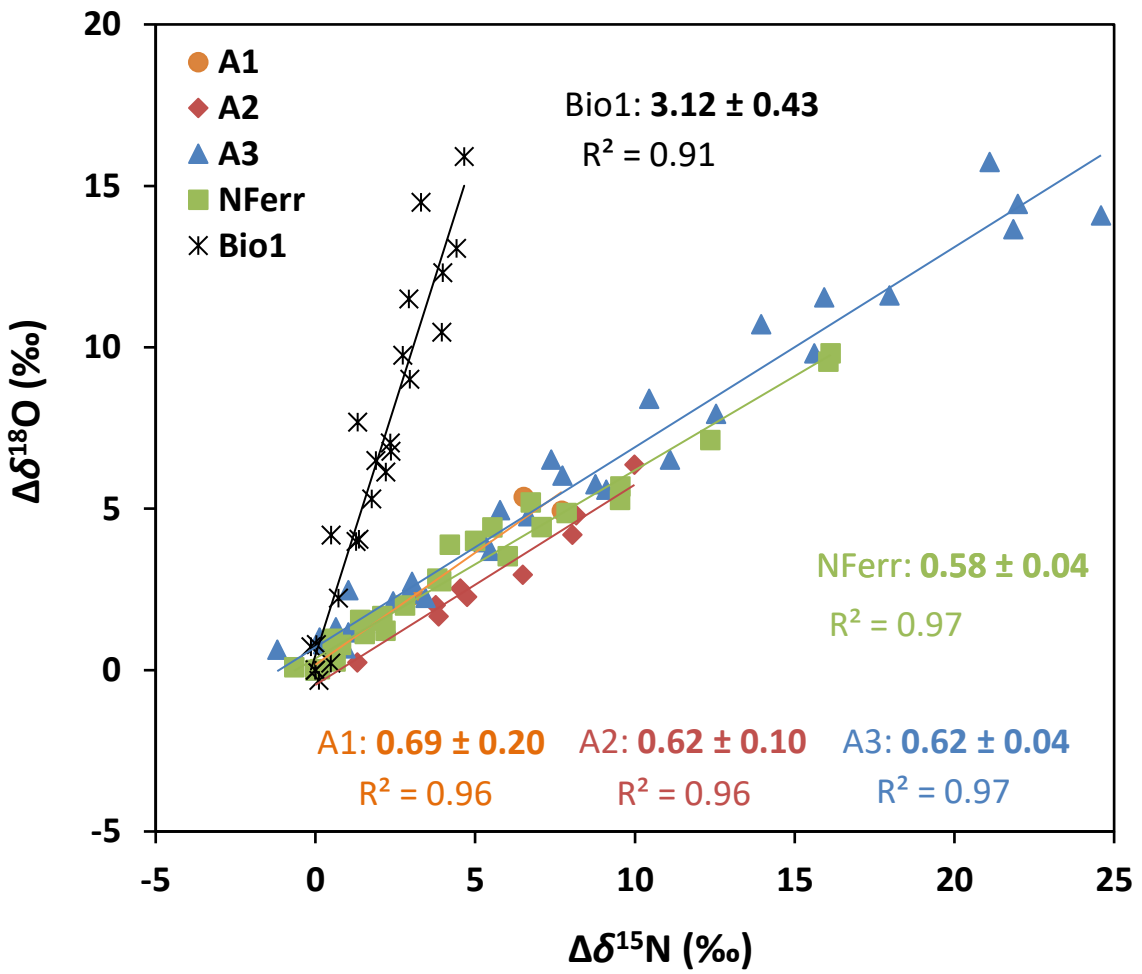


Figure 5

